www.MaterialsViews.com

Antimicrobial Materials

Ultrafast Killing and Self-Gelling Antimicrobial Imidazolium Oligomers

Siti Nurhanna Riduan, Yuan Yuan, Feng Zhou, Jiayu Leong, Haibin Su, and Yugen Zhang**

Infectious diseases and the increasing threat of worldwide pandemics have underscored the importance of antibiotics and hygiene. Intensive efforts have been devoted to developing new antibiotics to meet the rapidly growing demand. In particular, advancing the knowledge of the structure–property–activity relationship is critical to expedite the design and development of novel antimicrobial with the needed potential and efficacy. Herein, a series of new antimicrobial imidazolium oligomers are developed with the rational manipulation of terminal group's hydrophobicity. These materials exhibit superior activity, excellent selectivity, ultrafast killing (>99.7% killing within 30 s), and desirable self-gelling properties. Molecular dynamic simulations reveal the delicate effect of structural changes on the translocation motion across the microbial cell membrane. The energy barrier of the translocation process analyzed by free energy calculations provides clear kinetic information to suggest that the spontaneous penetration requires a very short timescale of seconds to minutes for the new imidazolium oligomers.

1. Introduction

Due to the global threat of pandemics and infectious diseases and its far-reaching consequences, there has been much research and development in the discovery of new antibiotics. Antimicrobial peptides (AMP) have attracted tremendous attention as an alternative to traditional antibiotics. AMPs exhibit selective membrane disruption activity, demonstrating a fast killing mechanism and the potential to deal with drug-resistance issues usually associated with conventional antibiotics.[1–5] However, the high cost of manufacture and poor in vivo half-lives of AMPs have limited its applications in healthcare and hygiene. To circumvent the limitations of AMPs as an antimicrobial material, the syntheses of disinfecting polymer constructs have seen much development.[6–10] Their structural characteristics are similar to that of AMPs, in which a fine balance of charge, typically stemming from the attachment of quaternary ammonium salts, and hydrophobicity, from long alkyl side-chains, ascertains their efficacy and selectivity as an antimicrobial.[11–15] These synthetic polymers possess the vast structural diversity that can be obtained via multistep organic synthesis, for ease of tuning the final amphiphilicity of the polymer, which will then dictate their selectivity and efficacy.[11–16]

As compared to the side-chain brush structure of most synthetic antimicrobial polymers, polymers with linear structures with all functional groups present in the main-chain, have also attracted much attention. Our group have recently reported the synthesis and application of imidazolium main-chain polymers/oligomers, AMP mimics, as efficient antimicrobials and antifungal treatment.[17,18] The imidazolium

Dr. S. N. Riduan, Dr. Y. Yuan, J. Leong, Dr. Y. Zhang
Institute of Bioengineering and Nanotechnology
31 Biopolis Way
The Nanos, Singapore 138669, Singapore
E-mail: ygzhang@ibn.a-star.edu.sg
Dr. F. Zhou, Prof. H. B. Su
School of Materials Science and Engineering
Nanyang Technological University
50 Nanyang Avenue, Singapore 639798, Singapore
E-mail: hbsu@ntu.edu.sg

DOI: 10.1002/smll.201600006

oligomers possess a well-designed chain structure, in which their amphiphilicity could be adjusted by changing the linking or end groups. In this paper, we present a strong correlation between the structure of the imidazolium oligomers and their properties and activities. By tuning their amphiphilic structure, the novel imidazolium oligomers demonstrate ultraefficient antimicrobial activities. The new material can selectively kill bacteria instantly without inducing hemolysis, even at much higher concentrations. The translocation process of imidazolium oligomers across the membrane was studied in detail by molecular-dynamics (MD) simulations. With the well-balanced amphiphilic structure, these materials are also able to self-assemble to form gels in alcohols. The interesting properties of these novel imidazolium materials suggest excellent potential in its use as an antimicrobial agent, particularly in common hygiene, sterilization, and other health care applications.

2. Results and Discussion

2.1. Novel Imidazolium Oligomers

For the previously reported imidazolium oligomer **IBN-1** (**Figure 1**), its amphiphilicity is dominated by polar segments (the calculated Partition Coefficient log$P_{o/w}$ is –6.14 and total polar surface area (TPSA) is 52.91). To further understand the killing mechanism, and consequently tuning the property and activity, we modified the structure of **IBN-1** by introducing more hydrophobic n-alkyl chains at the terminal ends. It was hypothesized that the long *n*-alkyl chains would trigger self-assembly processes, modify, or enhance the interaction between the compound and cell membrane, and may therefore enhance antimicrobial activity.

As shown in Figure 1, the terminal group of original imidazolium oligomer was changed from benzyl to cyclohexylmethyl (**IBN-Cy**) and linear n-alkyls (n = 6 to 16). As a consequence, the amphiphilicity of these materials have dramatically changed, as the calculated $logP_{O/W}$ value varied from –6.06 (**IBN-Cy**) to 0.27 (**IBN-C16**) (Table S1, Supporting Information). The oligomers' antimicrobial activities were then evaluated against four different and clinically relevant microbes: *S. aureus*, *E. coli*, *P. aeruginosa*, and *C. albicans*. The minimal inhibition concentration (MIC) values of all seven oligomers synthesized are presented in Figure 1 and Table S1 (Supporting Information). The MIC values of all these oligomers are in the low ppm range. As a comparison, we also tested the MICs of conventional antimicrobial agents that are currently in use in clinical treatment, such as chlorhexidine for *E. Coli*, vancomycin for *S. aureus*, and amphotericin B for *C. albicans*.

2.2. Structure–Property Relationship

Imidazolium oligomers demonstrated better or comparable antimicrobial activities against these microbes (Table S2, Supporting Information). Before these materials can be used in systemic applications, selectivity of these materials for microbial cells over mammalian cells should be considered. Such selectivity was often determined by observation of hemolysis. It was noted that hemolysis of red blood cells was not induced at the respective MIC values, for all the oligomers synthesized. The selectivity of the materials was also further assessed by calculating the selectivity indices (Figure S1, Supporting Information), a measure and a comparison of safety and efficacies of each oligomer analogue. The selectivity index of each oligomer was calculated as the ratio of HC_{10} value (defined as the lowest oligomer concentration that induces 10% or more hemolysis) to the GM (geometric mean of the MICs of the four microbes tested[19]). A high selectivity index or therapeutic index is preferable in order for a drug to be viewed as having a favorable safety profile.[20] As seen in Table S1 (Supporting Information), only the shorter chain analogues of **IBN-C6**, **IBN-C8**, **IBN-C10,** and **IBN-Cy** met this requirement. As shown in Figure 1, the MIC values increased with the length of the alkyl

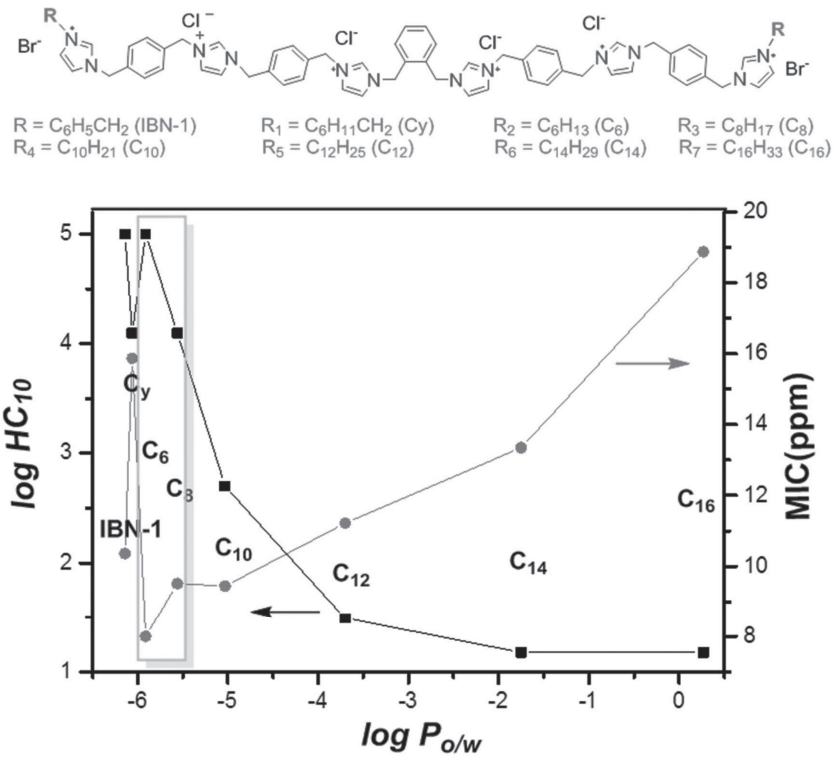

Figure 1. Molecular structures of imidazolium oligomers and the relationships among log *P*, log HC_{10}, and MIC (geometric mean of the MICs of the four microbes tested in ppm) of oligomers. **IBN-C6** and **IBN-C8** (in gray box) are the optimal candidates with the highest potency, while resulting in minimal hemolysis.

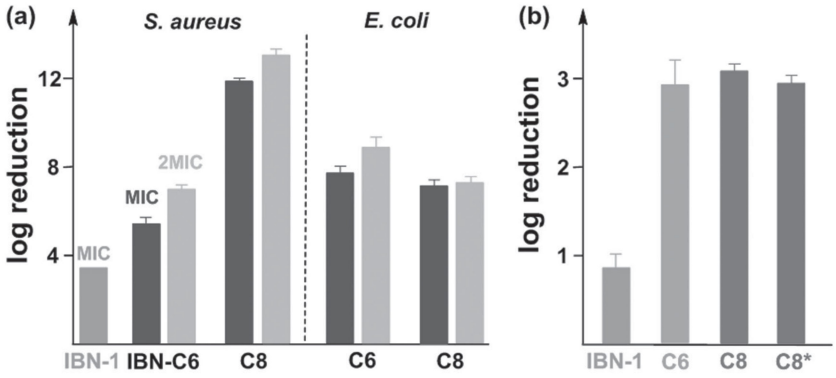

Figure 2. a) 24 h killing efficiency for **IBN-C6** and **C8** (MIC and 2MIC) against *S. aureus* and *E. coli*; b) 2 min (**C8*** = 30 s) killing efficiency for oligomers against *E. coli* at 32 mg mL^{-1}.

chain length. At the same time, the hemolytic ability of these materials also increased with the alkyl chain length. These observations correlate well with the calculated polarities. The exception of **IBN-Cy** also indicates that the properties of these imidazolium oligomers are highly dependent on the structure of the terminal groups. It has been well reported that biomolecules of higher hydrophobicity are generally more potent as a biocide, but are concurrently more toxic. However, for our current imidazolium oligomers, the molecules with longer hydrophobic tails exhibit less potency against various microbes, which reflect their lower solubility in water. From Figure 1, the compounds **IBN-C6** and **IBN-C8** highlighted in the blue box are the optimal candidates with the highest potency, while resulting in minimal hemolysis.

2.3. Fast Killing Property

While MIC values provide a perspective of the efficacy of a compound as an antimicrobial, it does not distinguish the compound's ability to either inhibit the growth of microbes, or eliminate the microbes completely. A compound is usually considered bactericidal if the minimum biocidal concentration (MBC) is less than four times the MIC value.[21] **IBN-C6** and **C8** analogues were further selected for MBC test. As shown in **Figure 2**a, **IBN-C6** and **C8** exhibited clear bactericidal behavior, in which more than 99.999% killing of microbes were attained when treated with the respective MIC concentrations for 24 h.

Time kill studies of the imidazolium oligomers and two active components (benzalkonium chloride and chloroxylenol) of common hygiene products against *E. coli* were also studied, and it was surprising that the imidazolium oligomers demonstrated superior ultrafast-killing property with **IBN-C8** having the best performance (Figure 2b; Figure S2, Supporting Information). More than 99.9% killing was observed within 2 min at 32 ppm concentration of **IBN-C8**, as compared to 83% killing for **IBN-1**. **IBN-C8** can also effectively kill *E. coli* in 30 s with a *log* reduction of 2.85. As shown in scanning electron microscopy (SEM) images, cell wall became disrupted and subsequently dissolved after 2 min exposure to **IBN-C8** (**Figure 3**). To further investigate the phenomena, positive control experiments with 1-Methyl-3-octyl imidazolium bromide (monomeric imidazolium with **C8** alkyl chain) were performed. MIC studies on 1-Methyl-3-octyl imidazolium bromide revealed a MIC value of 1000 ppm, more than 100 times of the **IBN-C8** analogue. Most of previously reported fast killing antimicrobials, such as AMPs and modified silver nanoparticles, exhibited microbe killing in a time scale of minutes to hours.[1–10,22,23] Such ultrafast-killing kinetics with simple oligomers or polymers has yet to be reported. From these observations, it can be deduced that the hydrophobic aliphatic chains do contribute to the advantageous instantaneous killing, in which the facial combination of hydrophobic end groups and the multiply charged imidazolium oligomer chain is the key structure-activity feature for this ultraefficient ultrafast killing behavior. In contrast, monomeric imidazolium salts with simple alkyl chains are ineffective and lack antimicrobial activities.

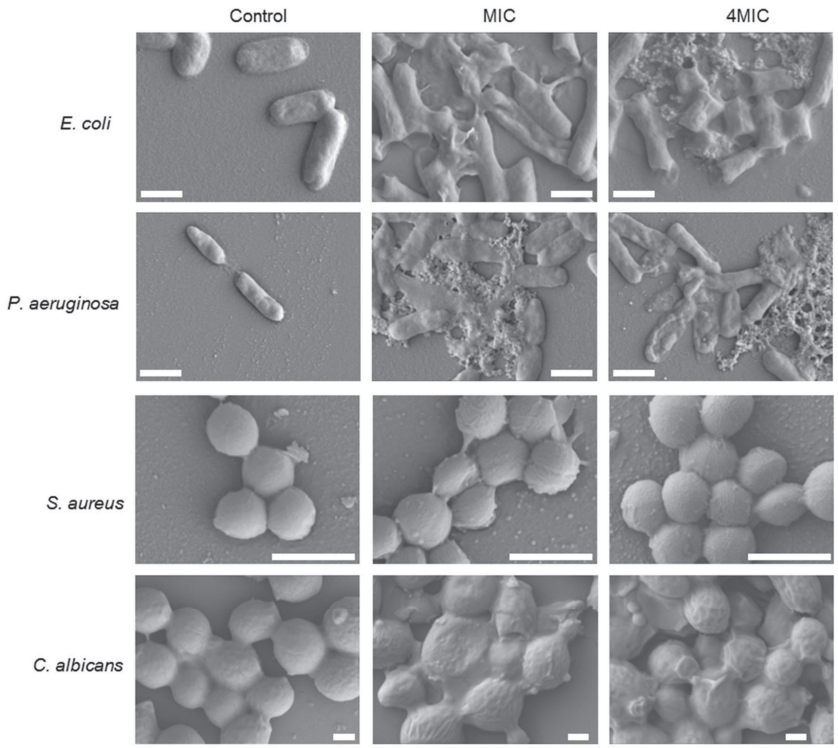

Figure 3. SEM images **IBN-C8** treated *E. coli, P. aeruginosa*, *S. aureus*, and *C. albicans* at MIC and 4MIC for short period. The treatment for *E. coli, P. aeruginosa*, and *S. aureus* is 2 min while for *C. albicans* is 2 h. Cell wall became disrupted and dissolved after exposure. Scale bars represent 1 μm.

2.4. Computational Study

Cationic compounds and polymers, in general, have the ability to perturb the lipid membranes of microbes through electrostatic and hydrophobic interactions with membrane phospholipids. This leads to membrane permeability, progressive leakage of cytoplasmic materials and consequential lysis of the cell.[1,24–26] Although mechanisms of cell-penetrating peptides have been well studied, the interaction of cationic polymers with cell membrane has rarely been examined.[27,28] The ultrafast-killing activity of **IBN-C8** against common microbes attracted our attention and we further probed the interaction between the alkyl terminal group and the cell membrane. To investigate such structure-property-activity effect, we utilized molecular dynamic (MD) simulations and umbrella-sampling techniques to compute free energy of the insertion of an imidazolium oligomer into 1-Palmitoyl-2-oleoyl-sn-glycero-3-phosphocholine (POPC) bilayer.[29] Specifically, the spontaneous binding of single and multiple motifs to POPC bilayer were studied together with the potential of mean force (PMF) associated with the translocation of **IBN-1**/**IBN-C8** through the membrane (Figures S3–S6, Supporting Information). From PMF study it was found that the oligomer did induce dramatic changes in the structure of the membrane (Figure S6, Supporting Information). The PMFs obtained from a combination of "pulling" and umbrella-sampling simulations provide strong evidence that the approach and penetration of the compound to the cell membrane is much easier for **IBN-C8** than for **IBN-1** (**Figure 4**).

To study the spontaneous binding of the oligomers to a lipid bilayer, as well as the potential for the oligomers to induce the formation of pores, a series of MD simulations of different conditions (using different initial structures) were performed. Starting from an equilibrated POPC bilayer containing 128 lipids, a series of six **IBN-1** (X = Cl) were added spontaneously, close to one side of the bilayer. However, no signs of spontaneous pore formation were observed within 200 ns. For the first 10 ns, the oligomers diffused on the surface of the membrane, with observable interactions with phosphate groups (Figure S3, Supporting Information). This adhesive process generated considerable stress gradually, which led the bending and slight thinning of the membrane starting from the subsequent 20 ns.[30] The early stages of oligomer insertion into the membrane were observed (Figures S4 and S5, Supporting Information). The terminal group of oligomer slowly diffuses to a region beneath the phosphate groups at the interface with the carbon chains of the lipids. The hydrophobic interactions provide the driving force to insert the terminal group into the more hydrophobic center region.

To reveal the kinetic information of the translocation process, we computed the free energy along the translocation pathway by applying a harmonic restraining potential between the center of mass of a single oligomer and the center of mass of the membrane, which was then moved at a rate of 0.1 nm ns^{-1} in the direction normal to the plane of the membrane, using the umbrella integration technique [31,32] are shown in Figure 4 and Figure S6 (Supporting Information). The free energy profiles are plotted from just before the center of the membrane (Z = 0 nm) to where the oligomer is surrounded by bulk solvent and no longer interacts directly with the bilayer (Z = 3.2 nm). The overall shapes of the free energy profile are similar for both molecules. There is a maximum in the free energy profile close to the center of the bilayer (Z = 0 nm) and a shallow

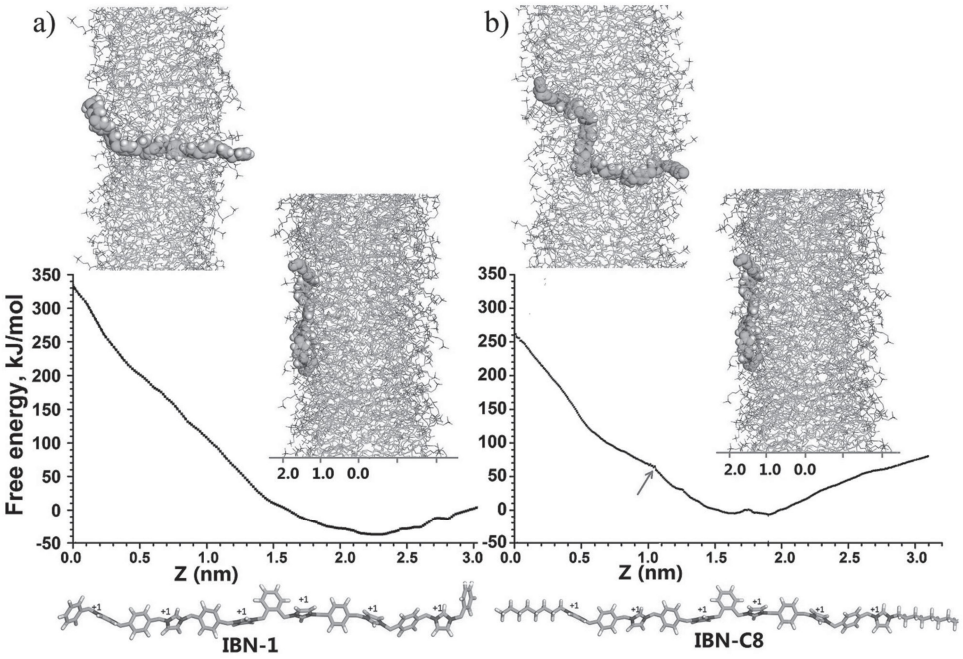

Figure 4. The free-energy of the translocation of a) **IBN-1** and b) **IBN-C8** through a POPC bilayer computed using the umbrella integration technique.[28] Z = 0 nm corresponds to the center of the membrane. The shallow minimum (Z = 2.0–2.5 nm) corresponds to where the molecule is interacting with the bilayer-water interface. A kink (denoted by an arrow) in the free-energy profile of **IBN-C8** is around 1.0 nm (interfacial region of membrane). The POPC lipids are shown as sticks and the oligomers are shown as spheres. The explicit water and counter ions are omitted for clarity.

minimum (Z = 1.5–2.5 nm) corresponding to where the molecule is interacting with the bilayer-water interface. The free-energy barrier to translocation is consistently lower for **IBN-C8** than for **IBN-1**. First, when motifs are at the center of POPC membrane, the system reaches the highest energy 330 kJ mol^{-1} for **IBN-1** and 260 kJ mol^{-1} for **IBN-C8**. This is anticipated, as the higher number of carbon atoms at the terminal end of **IBN-C8** makes it lower in energy when it is in the center of the membrane, due to stronger hydrophobic interactions. Second, the reduction in free energy when the oligomer moves from the solution phase to the surface of the lipid bilayer is larger for **IBN-C8** than for **IBN-1** (energy profiles from 3.1 nm to shallow minimum: –80 kJ mol^{-1} for **IBN-C8** and –38 kJ mol^{-1} for **IBN-1**), indicating that the terminal C_8H_{17} chain in **IBN-C8** disfavors water more than the terminal benzyl group in **IBN-1**. The minimum valley in the free energy profile for **IBN-C8** (Z = 1.5–.0 nm) is closer to the interfacial region of the membrane (Z = 1.0 nm) as compared to **IBN-1** (Z = 2.0–2.5 nm).

Another feature of importance in Figure 4 is a kink (denoted by a red arrow) in the free energy profile of **IBN-C8** around 1.0 nm (interfacial region of membrane), which becomes more pronounced as the system is equilibrated.[33] This kink represents the energy barrier (65 kJ mol^{-1}) associated with the oligomer crossing the interfacial region and the formation of the transmembrane pore. The kink indicates that as the C8 chain of **IBN-C8** crossing the interfacial region, the strong hydrophobic interactions between C8 chain and the hydrophobic center of membrane allows for easier penetration of the rest of the oligomer to the interfacial region. This free energy (65 kJ mol^{-1}) for the insertion of **IBN-C8** into a POPC bilayer suggests that the spontaneous penetration of **IBN-C8** would take place in a timescale of seconds to minutes.[34] This is consistent with its ultrafast-killing property as observed in our experimental work. For **IBN-1**, there is no clear kink observed, probably due to the absence of strong hydrophobic groups. The free energy of **IBN-1** crossing interfacial region (1.0 nm) is about 140 kJ mol^{-1}, which is much higher than **IBN-C8**. In all, energy profiles of Figure 4 indicate that it is easier for **IBN-C8** to approach the cell membrane, to lie on the central region of the membrane and to form the transmembrane pore, as compared to the **IBN-1**.

2.5. Self-Gelation

The introduction of long n-alkyl chains will render the molecules amphiphilic, and we hypothesize that this would trigger self-assembly processes. It has been reported that enhanced microbial action was observed with prior microstructure formation of polymer into micelles prior to treatment of microbes.[35] Most amphiphilic molecules are able to form micelles in aqueous solutions, and for some antimicrobial compounds, such self-assembly were critical to their efficacy. The synthesized **IBN-1** analogues, having a structures consisting of a hydrophobic tails attached both ends of a hydrophilic block were then studied for their ability to form micellar microstructures. It was observed that the only oligomers with the long hydrophobic n-alkyl chains of **IBN-C12** to **C16** were able to form micelles. Such oligomers form micelles at concentrations lower than that of the MIC values in PBS solution, where the **IBN-C12**, **C14**, and **C16** oligomers were able to form micelles at 10.9, 4.9, and 1.3 ppm, respectively (Table S3, Supporting Information). In comparison, a sharp point of inflection indicating the critical micellar concentrations was not observed for the shorter chain analogues, **IBN-C6**, **C8**, **C10**, and the original **IBN-1** oligomer (Figure S7, Supporting Information). This could mean that these oligomers exist freely in solution, with fleeting aggregations due to nonspecific interactions. More significantly, it revealed that micellar microstructure formation of the oligomers was not essential to antimicrobial action. In fact, the longer chain oligomers often had higher MIC values than that of the shorter chains and the original **IBN-1**.

In the process of further examining the self-assembly properties of these amphiphilic chains,[36] it was found that the **IBN-C16** oligomer was able to form opaque gels in solvents that are frequently used in general disinfection applications, such as glycerol and ethylene glycol. While **IBN-C12** oligomer did not form gels in binary mixtures of water/ethanol and glycerol/ethanol, we were pleasantly surprised that the oligomers were able to form gels in pure ethanol at a concentration of less than 10 wt%. We expanded the gelling ability studies to all the oligomers in the series and various alcohols, and were delighted that all the oligomers were able to form opaque gels in ethanol, n-propanol and n-butanol (Table S4, Supporting Information). For IBN-C8, it showed moderate gelation ability in ethanol, *n*-propanol, and *n*-butanol with the CGC in the range of 2.0 to 4.0 wt% (Table S5, Supporting Information). It must be noted that both **IBN-1** and **Cy** oligomers were not able to form gels in any of the solvents, and no gels were formed with the use of branched alcohols of isopropanol and tert-butanol.

While gels were stable at ambient temperatures, it was observed that the gels were thixotropic; in which when the vials containing the gels were vortexed, it becomes fluid but consequently sets into a solid-like state in the course of a few minutes. Rheology characterization revealed that the gels are indeed weak gels, with low G′ value, and the viscosity of the gels decreased with increasing shear rate, indicating thixotropic behavior (Figures S8 and S9, Supporting Information).[37] To determine the range of linear viscoelastic behaviour, we performed strain-amplitude sweeps on the gels of **IBN-C8** in the selected alcohols. All gels exhibited elastic responses. The storage moduli G′ decrease rapidly above critical strains of 10%–90%, indicating a strain-induced collapse of the gel state (Figure S10, Supporting Information). The critical strain of the tested gels depends on the type of alcohol. Accordingly, the angular frequency sweep experiments were performed at 5% strain. The obtained storage moduli G′ and loss moduli G″ of the gels of **IBN-C8** in different alcohols are plotted against the frequency (Figure S11, Supporting Information). The G′ was constantly higher than G″ for the entire range of frequencies, which means all the gels are dominated by their elastic properties. All gels display thermal reversibility. They melt upon heating and turned back into gel upon cooling to room temperature. The storage and loss moduli of **IBN-C8** in EtOH (11.0%), n-PrOH

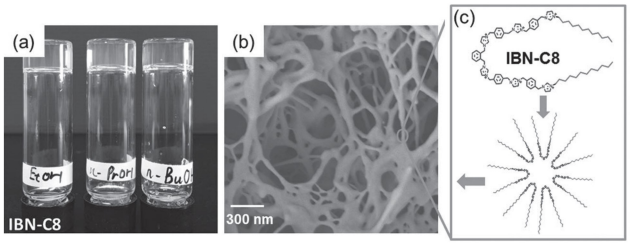

Figure 5. a) Image of **IBN-C8** gels formed in EtOH (11.0%), *n*-PrOH (9.8%), and *n*-BuOH (5.5%); b) SEM image of **IBN-C8** gel in *n*-butanol; and c) their self-assembly process.

(9.8%), and n-BuOH (11.3%) measured from a temperature ramp performed at 5% strain were shown in Figure S12 (Supporting Information). The gel of IBN-C8 in EtOH is only stable when the temperature is lower than 35 °C while the gels formed in n-PrOH and n-BuOH were stable in the tested range from 25 to 50 °C (Figure S12, Supporting Information). SEM imaging was done on the **IBN-C8** xerogels, and it was observed that these gels had a spongy nature to them, see **Figure 5**. This led us to believe that these are likely to be fluid matrix organogels, in which the only forces holding them together are simple chain entanglements. This is in agreement with the fact that **IBN-1** and **IBN-Cy** cannot form gels in linear alcohols, while **IBN-C6** to **IBN-C16** cannot form gels in branched alcohols. These amphiphilic structures are postulated to form loose aggregations at low concentrations, and at higher concentrations, form fibrillar networks that are intertwined in the solvent mix, trapping the solvent in the matrix.

It is well known that many amphiphilic structures, such as block-co-polymers and peptides, could form gels via self-assembly to certain microstructures.[37,38] While most of antimicrobial materials can assume amphiphilic structures, self-gelations are seldom realized. There have been reports of antimicrobial materials that can assemble to hydrogels including peptides[39] and block polymers based on chitin[40] and lactic acid[41] materials. However, these assembly processes are typically triggered by cogelation polymers or grafting antimicrobial material with other polymers. Here, the unique sandwich-type amphiphilic structure of **IBN-C6–IBN-C16** imidazolium oligomers provides novel properties including highly active antimicrobial activities and the added ability to self-assemble to organogels, Figure 5c. A standard zone of inhibition test under static conditions was performed to evaluate the antimicrobial activity of the gels (Figure S13, Supporting Information). The zone of inhibition for n-BuOH is about 7 mm, while the zone of inhibition for **IBN-C8**/n-BuOH gel is 23 mm. The antimicrobial activity of the **IBN-C8** gel is significantly higher than the antimicrobial activity of the solvent alone, implying that the antibacterial property of the imidazolium oligomers is retained after they form gels in the alcohol. These properties are especially attractive for applications in personal hygiene, sterilization, and other health care areas.

3. Conclusion

We have synthesized a series of imidazolium oligomers with a range of terminal alkyl groups. By varying the length of alkyl chain of the terminal groups we were able to study the structure–property–activity relationship. In the oligomer series, it was observed that the **IBN-C8** oligomer possesses extremely high killing activity against common microbes, without being toxic. The excellent efficiency was due to the fine balance of the hydrophobic and hydrophilic regions, allowing for better interaction and penetration to the bacterial wall membrane. This observation was further supported by computational chemistry studies. In addition, it was also found that the oligomers were able to form gels spontaneously in common alcoholic solvents. These results indicate the high potential of the applicability of these oligomers as a consumer antimicrobial product.

4. Experimental Section

All materials were purchased from Sigma Aldrich or Merck, and used as purchased. All manipulations were done without any special precautions to eliminate air or moisture. Synthesis of imidazolium oligomers were adapted from protocols reported previously.[17,42] See supporting information for more details.

Minimum Inhibitory Concentration: *Staphylococcus aureus* (ATCC 6538, Gram-positive), *Escherichia coli* (ATCC 25922, Gram-negative), *Pseudomonas aeruginosa* (ATCC 15442, Gram-negative), and *Candida albicans* (ATCC 10231, fungus) were used as representative microorganisms to challenge the antimicrobial functions of the imidazolium salts. All bacteria and fungus were stored frozen at –80 °C, and were grown overnight at 37 °C in Tryptic Soy broth (TSB) prior to experiments. Fungus was grown overnight at 22 °C in Yeast Mold (YM) broth. Subsamples of these cultures were grown for a further 3 h and diluted to give an optical density value of 0.07 at 600 nm, corresponding to 3×10^8 CFU mL^{-1} (McFarland' Standard 1).

Time Kill Kinetics: The experimental setup for time kill kinetics was similar to the set up for MBC determination. The microbes were treated with oligomers at 4MIC concentration, and samples were taken out of each well at 2 min. 500 µl of cell suspension was removed, rescued by a series of tenfold dilutions with growth medium, and kept on ice until plating. For plating, 50 to 200 µl of the diluted samples was spread on growth medium agar plates and colonies were counted after overnight incubation at 37 °C.

Computational Study: All simulations were performed using the GROMACS 4.5.3 suite of programs.[43] The GROMOS 53a6 force field[44] was used to describe the oligomer, and the lipids were described using the parameters of Berger et al.[45] Water molecules were described using the TIP3P water model.[46] All simulations were performed under periodic boundary conditions at constant temperature and pressure.

Supporting Information

Supporting Information is available from the Wiley Online Library or from the author.

Acknowledgements

*S.N.R., Y.Y., and F.Z. contributed equally to this work. This work was supported by the Institute of Bioengineering and Nanotechnology, Biomedical Research Council, Joint Council Office, SERC Personal Care Programme, and Agency for Science, Technology and Research. The authors thank A*STAR Computational Resource Centre for the use of its high performance computing facilities.*

[1] M. Zasloff, *Nature* **2002**, *415*, 389.
[2] S. Fernandez-Lopez, H. S. Kim, E. C. Choi, M. Delgado, J. R. Granja, A. Khasanov, K. Kraehenbuehl, G. Long, D. A. Weinberger, K. M. Wilcoxen, M. R. Ghadiri, *Nature* **2001**, *412*, 452.
[3] R. E. W. Hancock, H. G. Sahl, *Nat. Biotechnol.* **2006**, *24*, 1551.
[4] G. Bell, P. H. Gouyon, *Microbiology* **2003**, *129*, 15615.
[5] J. G. Hurdle, A. J. O'Niell, I. Chopra, R. E. Lee, *Nat. Rev. Microbiol.* **2011**, *9*, 62.
[6] K. M. G. O'Connell, J. T. Hodgkinson, H. F. Sore, M. Welch, G. P. C. Salmond, D. R. Spring, *Angew. Chem. Int. Ed.* **2013**, *52*, 10706.
[7] G. N. Tew, R. W. Scott, M. L. Klein, W. F. DeGrado, *Acc. Chem. Res.* **2010**, *43*, 30.
[8] A. C. Engler, N. Wiradharma, Z. Y. Ong, D. J. Coady, J. L. Hedrick, Y.-Y. Yang, *Nano Today* **2012**, *7*, 201.
[9] A. Tello, B. Austin, T. C. Telfer, *Environ. Health Perspect.* **2012**, *120*, 1100.
[10] A. Munoz-Bonilla, M. Fernandez-Garcia, *Prog. Polym. Sci.* **2012**, *37*, 281.
[11] K. Kuroda, W. F. DeGrado, *J. Am. Chem. Soc.* **2005**, *127*, 4128.
[12] S. Chakraborty, R. Liu, Z. Hayouka, X. Chen, J. Ehrhardt, Q. Lu, E. Burke, Y. Yang, B. Weisblum, G. C. L. Wong, K. S. Masters, S. H. Gellman, *J. Am. Chem. Soc.* **2014**, *136*, 14530.
[13] M. F. Ilker, K. Nüsslein, G. N. Tew, E. B. Coughlin, *J. Am. Chem. Soc.* **2004**, *126*, 15870.
[14] B. Gao, X. Zhang, Y. Zhu, *J. Biomater. Sci., Polym. Ed.* **2007**, *18*, 531.
[15] N. Pasquier, H. Keul, E. Heine, M. Moeller, *Biomacromolecules* **2007**, *8*, 2874.
[16] F. Nederberg, Y. Zhang, J. P. K. Tan, K. Xu, H. Wang, C. Yang, S. Gao, X. D. Guo, K. Fukushima, L. Li, J. L. Hedrick, Y.-Y. Yang, *Nat. Chem.* **2011**, *3*, 409.
[17] L. Liu, Y. Huang, S. N. Riduan, S. Gao, Y.-Y. Yang, W. Fan, Y. Zhang, *Biomaterials* **2012**, *33*, 8625.
[18] L. Liu, H. Wu, S. N. Riduan, J. Y. Ying, Y. Zhang, *Biomaterials* **2013**, *34*, 1018.
[19] B. I. Davies, *J. Antimicrob. Chemother.* **1990**, *25*, 471.
[20] P. Y. Muller, M. N. Milton, *Nat. Rev. Drug Discovery* **2012**, *11*, 751.
[21] G. L. French, *J. Antimicrob. Chemother.* **2006**, *58*, 1107.
[22] J. M. Boyce, *Am. J. Infect. Control* **2013**, *41*, S94.
[23] A. E. Madkour, J. M. Dabkowski, K. Nüsslein, G. N. Tew, *Langmuir* **2009**, *25*, 1060.
[24] A. J. McBain, R. G. Ledder, L. E. Moore, C. E. Catrenich, P. Gilbert, *Appl. Environ. Microbiol.* **2004**, *70*, 3449.
[25] S. Wessels, H. Ingmer, *Regul. Toxicol. Pharmacol.* **2013**, *67*, 456.
[26] M. S. Ganewatta, Y.-P. Chen, J. Wang, J. Zhou, J. Ebalunde, M. Nagarkatti, A. W. Decho, C. Tang, *Chem. Sci.* **2014**, *5*, 2011.
[27] H. Leontiadou, A. E. Marks, S. J. Marrink, *J. Am. Chem. Soc.* **2006**, *128*, 12156.
[28] E. Matyus, C. Kandt, D. P. Tieleman, *Curr. Med. Chem.* **2007**, *14*, 2789.
[29] M. Ceccarelli, M. Marchi, *Biochemie* **1998**, *80*, 415.
[30] H. D. Herce, A. E. Garcia, *Proc. Natl. Acad. Sci. USA* **2007**, *104*, 20805.
[31] J. Kastner, W. Thiel, *J. Chem. Phys.* **2005**, *123*, 144104.
[32] C. L. Wee, A. Chetwynd, M. S. P. Sansom, *Biophys. J.* **2011**, *100*, 410.
[33] S. Yesylevskyy, S.-J. Marrink, A. E. Mark, *Biophys. J.* **2009**, *97*, 40.
[34] A. Babakhani, A. A. Gorfe, J. E. Kim, J. A. McCammon, *J. Phys. Chem. B* **2009**, *112*, 10528.
[35] L. Liu, K. Xu, H. Wang, J. P. K. Tan, W. Fan, S. S. Venkatraman, L. Li, Y.-Y. Yang, *Nat. Nanotechnol.* **2009**, *4*, 457.
[36] a) F. D'Anna, P. Vitale, S. Marullo, R. Noto, *Langmuir* **2012**, *28*, 10849; b) T. Tu, W. Assenmacher, H. Peterlik, G. Schnakenburg, K. H. Dötz, *Angew. Chem. Int. Ed.* **2008**, *47*, 7127; c) S.N. Riduan, Y. G. Zhang, *Chem. Soc. Rev.* **2013**, *42*, 9055; d) F. D'Anna, C. Rizzo, P. Vitale, G. Lazzara, R. Noto, *Soft Matter* **2014**, *10*, 9281.
[37] X. Du, J. Zhou, B. Xu, *Chem. Asian J.* **2014**, *9*, 1446.
[38] R. G. Weiss, *J. Am. Chem. Soc.* **2014**, *136*, 7519.
[39] D. A. Salick, J. K. Kretsinger, D. J. Pochan, J. P. Schneider, *J. Am. Chem. Soc.* **2007**, *129*, 14793.
[40] P. Li, Y. F. Poon, W. Li, H.-Y. Zhu, S. H. Yeap, Y. Cao, X. Qi, C. Zhou, M. Lamrani, R. W. Beuerman, E.-T. Kang, Y. Mu, C. M. Li, M. W. Chang, S. S. J. Leong, M. B. Chan-Park, *Nat. Mater.* **2011**, *10*, 149.
[41] C. Zhou, P. Li, X. Qi, A. R. M. Sharif, Y. F. Poon, Y. Cao, M. W. Chang, S. S. J. Leong, M. B. Chan-Park, *Biomaterials* **2011**, *32*, 2704.
[42] Y. Zhang, L. Zhao, P. K. Patra, D. Hu, J. Y. Ying, *Nano Today* **2009**, *4*, 13.
[43] D. van der Spoel, E. Lindahl, B. Hess, G. Groenhof, A. E. Mark, H. J. Berendsen, *J. Comput. Chem.* **2005**, *26*, 1701.
[44] C. Oostenbrink, A. Villa, A. E. Mark, W. F. van Gunsteren, *J. Comput. Chem.* **2004**, *25*, 1656.
[45] O. Berger, O. Edholm, F. Jahnig, *Biophys. J.* **1997**, *72*, 2002.
[46] W. L. Jorgensen, J. Chandrasekhar, J. D. Madura, R. W. Impey, M. L. Klein, *J. Chem. Phys.* **1983**, *79*, 926.

Received: January 2, 2016
Revised: January 9, 2016
Published online: February 17, 2016